



PAPER

A computer-assisted experiment to study the influence of the point spread function in the image formation process

To cite this article: Vicente Ferrando *et al* 2018 *Eur. J. Phys.* **39** 065301

View the [article online](#) for updates and enhancements.



IOP | ebooks™

Bringing you innovative digital publishing with leading voices to create your essential collection of books in STEM research.

Start exploring the [collection](#) - download the first chapter of every title for free.

A computer-assisted experiment to study the influence of the point spread function in the image formation process

Vicente Ferrando¹, Laura Remón², Isabel Salinas¹,
Juan A Monsoriu¹  and Walter D Furlan³

¹ Centro de Tecnologías Físicas, Universitat Politècnica de València, E-46022 Valencia, Spain

² Departamento de Física Aplicada, Universidad de Zaragoza, E-50009 Zaragoza, Spain

³ Departamento de Óptica y Optometría y Ciencias de la Visión, Universitat de València, E-46100 Burjassot, Spain

E-mail: walter.furlan@uv.es

Received 4 June 2018, revised 23 July 2018

Accepted for publication 24 August 2018

Published 15 October 2018



CrossMark

Abstract

We present a new open experimental setup assisted with LabView to be used to teach the concept of the point spread function (PSF). The PSF describes the response of an image-forming system to a point object. The PSF concept is of fundamental importance in optics since the output of an image-forming system can be simulated as the convolution of the PSF with the input object. In this work, a new graphical user interface has been developed to obtain a real-time measure of the PSF and the corresponding images provided by different lenses and pupils with different sizes and shapes. From a didactical point of view, the proposed method allows students to interpret the results in a visual and heuristic way.

Keywords: image formation, PSF, GUI

(Some figures may appear in colour only in the online journal)

1. Introduction

The image quality provided by image-forming systems is limited by their optical aberrations and by the diffraction phenomenon. Diffraction effects are associated with limited aperture size due to the wave nature of the light, and therefore are more noticeable with small pupils. On the other hand, the impact of optical aberrations on image quality is more significant for

larger pupil diameters [1]. The point spread function (PSF) is a widely used merit function in optics to assess the imaging properties of optical systems such as microscopes, telescopes and ophthalmic lenses [2–5]. The PSF determines the resolution of the optical system and is defined as the response of an image-forming system to a point object. The output image then becomes the convolution of the input image with the PSF [6, 7].

For a given optical system under plane-wave illumination, the PSF is the diffraction pattern provided by the system at the paraxial focal point. Therefore, it can be computed through a Fourier transform of the system pupil function. For unaberrated lenses with circular pupils, the corresponding diffraction pattern is the well-known Airy disc and it depends only on the pupil diameter, the focal length and the wavelength. Thus, small pupils increase the diffraction effects producing extended PSFs and reducing the resolving power of the image-forming system. On the other hand, for aberrated lenses, the PSF depends on the phase variations across the pupil function. Therefore, small pupils reduce optical aberrations and also extend the depth of focus (DOF), i.e. the distance range over which an object remains in focus for a fixed image detection plane [8].

Since the PSF is a fundamental concept in optical science and technology, it is a central topic in optics courses. Although the concept of the PSF is quite simple, it is derived through a complex valued function (with amplitude and phase); and, according to our teaching experience [9], to fully understand it, students need a way to examine the PSF of a given optical system (even a single lens) under different conditions (i.e. different pupil sizes and shapes, tilts and defocus, etc) and to see its influence in real images. To meet this need, we have implemented an experimental setup, made with standard equipment available in most undergraduate optics laboratories. The proposed open experimental setup is assisted with a developed LabView software. LabView is a very intuitive and visual programming language that, due to its ease of use and flexibility, is nowadays frequently used [10, 11]. We have developed a new graphical user interface (GUI), which allows students to obtain a fast measure of the PSF for different lenses and pupils with different sizes and shapes. The GUI also provides in real time a numerically simulated image of the input object provided by the system under investigation by performing a convolution of the input object with the PSF captured by the experimental setup.

2. Basic theory

The PSF of a general optical system (OS) is defined as the image of a point source as it is shown in figure 1 [6, 7]. The light distribution at the exit pupil of the OS, originated on the point source, is affected by the optical aberrations of the OS, described by the wave aberration function $W(x, y)$, which defines the phase of the wavefront at the exit pupil, and by the physical aperture defined by the transmittance of the exit pupil, $p(x, y)$. In mathematical terms, the PSF of a general OS under incoherent illumination can be expressed in terms of a Fourier transform of its generalized pupil function $p(x, y) \cdot \exp\left[-i\frac{2\pi}{\lambda}W(x, y)\right]$:

$$PSF(x, y) = \frac{1}{\lambda^2 d^2 A_p} \left\| FT \left\{ p(x, y) \cdot \exp\left[-i\frac{2\pi}{\lambda}W(x, y)\right] \right\} \right\|_{f_x = \frac{x}{\lambda d}, f_y = \frac{y}{\lambda d}}^2. \quad (1)$$

In equation (1) FT is the Fourier transform operator, f_x and f_y are the spatial frequencies at the image plane; d is the distance from exit pupil to the image plane (see figure 1), A_p is the area of the exit pupil, and λ is the wavelength. The term $\exp\left[-i\frac{2\pi}{\lambda}W(x, y)\right]$ accounts for the phase derivations of the wavefront from a spherical reference wavefront converging to the

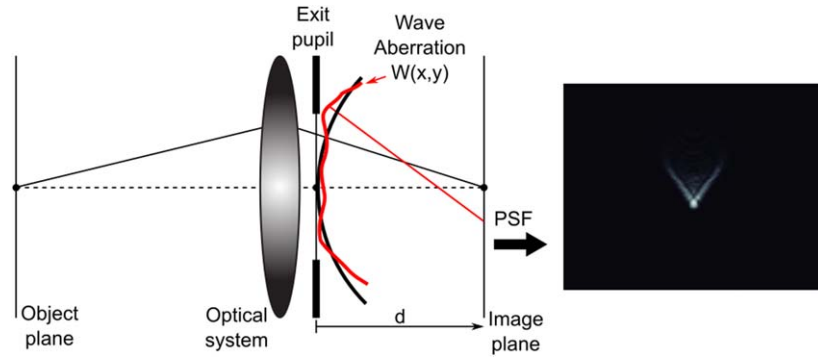


Figure 1. Schematic representation of a general imaging system.

geometrical optics image point. In this way, if the optical system is free from aberrations ($W(x, y) = 0$), the image of a point object is limited by the diffraction of the pupil amplitude. In the case of a circular aperture, the intensity pattern at the image plane is the well-known Airy pattern. The size of the disk depends on the aperture diameter, the focal length of the optical system and the wavelength of the light. However, real optical systems are not aberration free ($W(x, y) \neq 0$) and the wavefronts, which are surfaces of constant phase, deviate from sphericity. In this case, the size and shape of the PSF depends on the aberrations presents on the optical system (see figure 1). Using the PSF, the image $I(x, y)$ of a given object represented by the function $t(x, y)$ can be computed as [6]

$$I(x, y) = \frac{1}{M^2} \left| t\left(\frac{x}{M}, \frac{y}{M}\right) \right|^2 \otimes_2 PSF(x, y) \quad (2)$$

where M is the geometric optics magnification between the object and image planes and \otimes_2 represents the 2D convolution operator.

3. Experimental setup and data analysis

Figure 2 shows the experimental setup developed for the visualization and analysis of the PSF. A $30 \mu\text{m}$ pinhole, acting as a quasi-point-like source, is illuminated with a laser diode of wavelength 650 nm . The pinhole is located at the focal plane of the collimator lens (L_C) to obtain a collimated wavefront. Two linear polarizers (LP) are used to control the amount of light reaching the CCD camera. The optical elements (OLs) to be tested (lenses, pupils, and any combination of them) are mounted on a rotary stage with an XY micrometer platform. Next, a lens (L_F) of 250 mm focal length is used to focus the beam at the camera sensor (EDMUND EO-5012C $1/2''$ CMOS, 2560×1920 pixels, $2.2 \mu\text{m}$ pixel width). The Lab-View-based GUI was aimed to display the PSF and, at the same time, to obtain the simulated image that the OL under test will provide for a given object. The camera exposure time and the threshold gray level (between 0 and 255) can be adjusted to optimize the dynamic range of the PSF image (i.e. to avoid saturated regions of the image and to define the useful PSF area). Finally, the captured image file is analyzed with the software following the flowchart shown in figure 3.

In addition to the on-line PSF captured by the camera and displayed on the screen, the user introduces the input parameters needed to compute the simulated image. The size of the PSF area is automatically detected by the program, cropped and shown in another window on

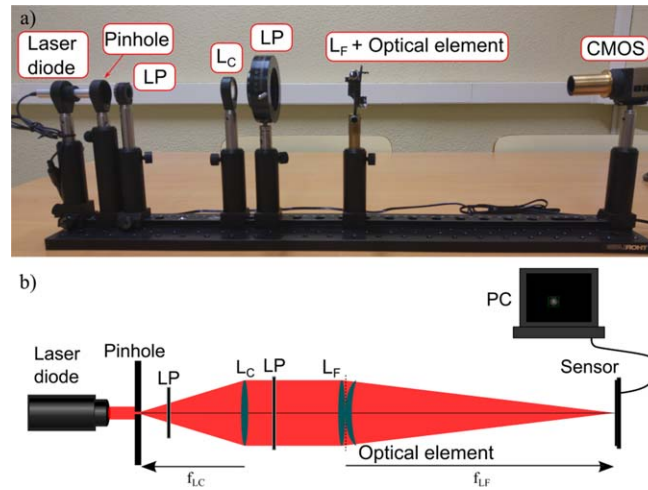


Figure 2. Experimental setup employed in the analysis of the PSF.

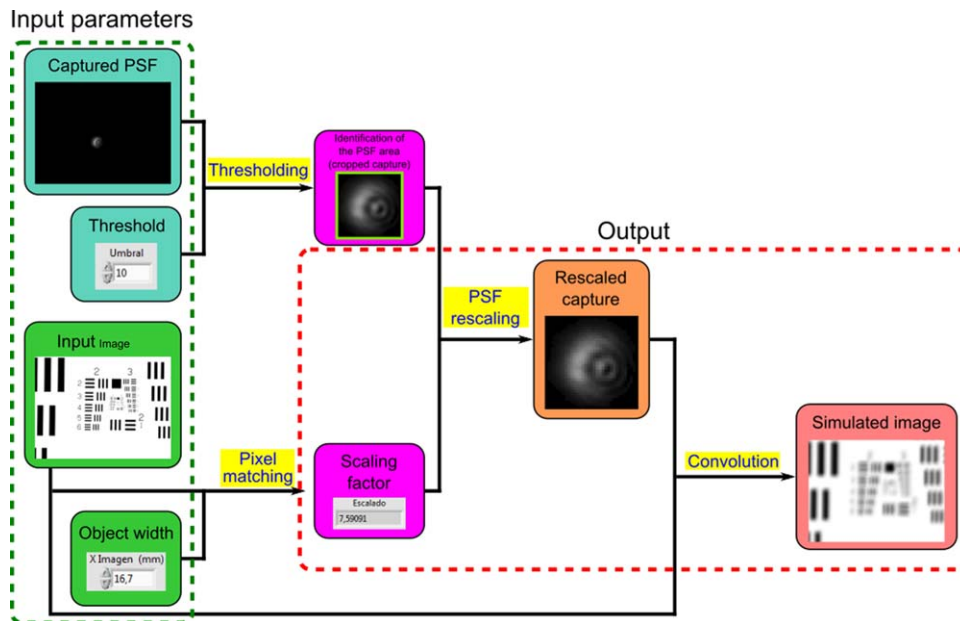


Figure 3. Flowchart of the proposed algorithm.

the screen in which a variable level of zoom can be selected to observe fine details of the PSF not perceived in the original image. An input image is then loaded from an image file and its resolution is defined in terms of another variable parameter, the object width in cm. This value defines the horizontal dimension used for the image simulation. With the input parameters, the scaling factor between the camera pixel size and the object pixel size is calculated in order to match them to perform the convolution represented by equation (2) (see figure 3). Finally, the GUI shows the loaded object, the captured PSF, the cropped and rescaled PSF, the scaling

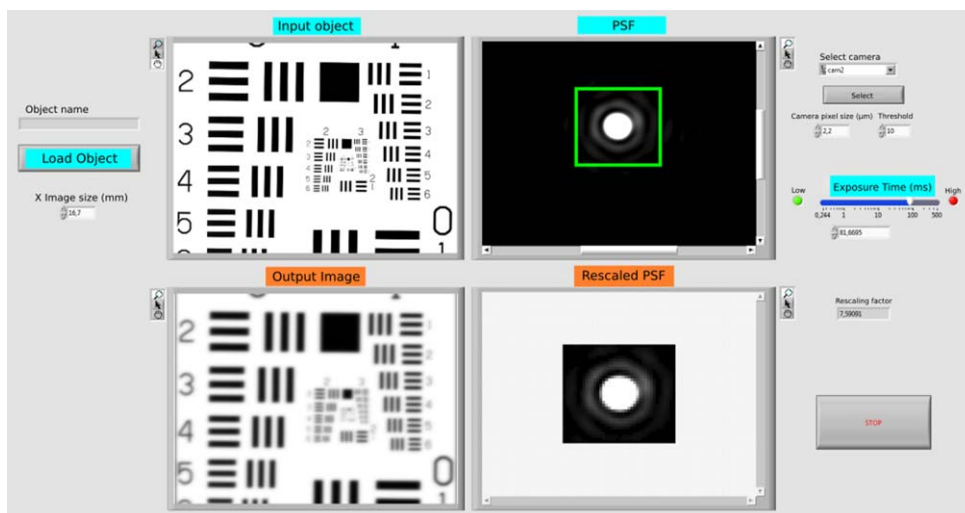


Figure 4. GUI main frame.

factor and the simulated image, as shown in figure 4. This software is available under request from the authors.

4. Results

In our laboratory teaching sessions, a set of lenses with different spherical and cylindrical powers and with different pupil types and sizes are analyzed. Three different experiments are described as follows.

4.1. Influence of defocus on the evolution of an astigmatic wavefront

Figure 5 shows the experimental PSF and the corresponding simulated image at three different positions corresponding to the main focal planes and at the circle of least confusion (located halfway between the two focal lines). At the oblique directions details of the object are sharper in the same directions of the corresponding PSF (compare the hat of 'Lena' in the images). At the circle of least confusion plane, the image is homogeneously blurred.

4.2. Influence on the image of different pupil shapes

Figure 6 shows the results obtained for the experimental PSF and the simulated images of a Siemens Star object. The PSF images are saturated in this figure to enhance the shape of the diffraction pattern. Again, it can be noticed that the simulated image is more blurred in the directions where the PSF is wider. Note also the inhomogeneous contrast reversal in the center of the star images. The green rectangle in the PSF shows the PSF area used in the convolution operation.

4.3. Depth of focus with different pupil sizes

Figure 7 shows the experimental PSF of a spherical lens with a pupil diameter of 12 mm and the same lens with a pupil of 2 mm. As can be seen, at the image plane the in-focus PSF for

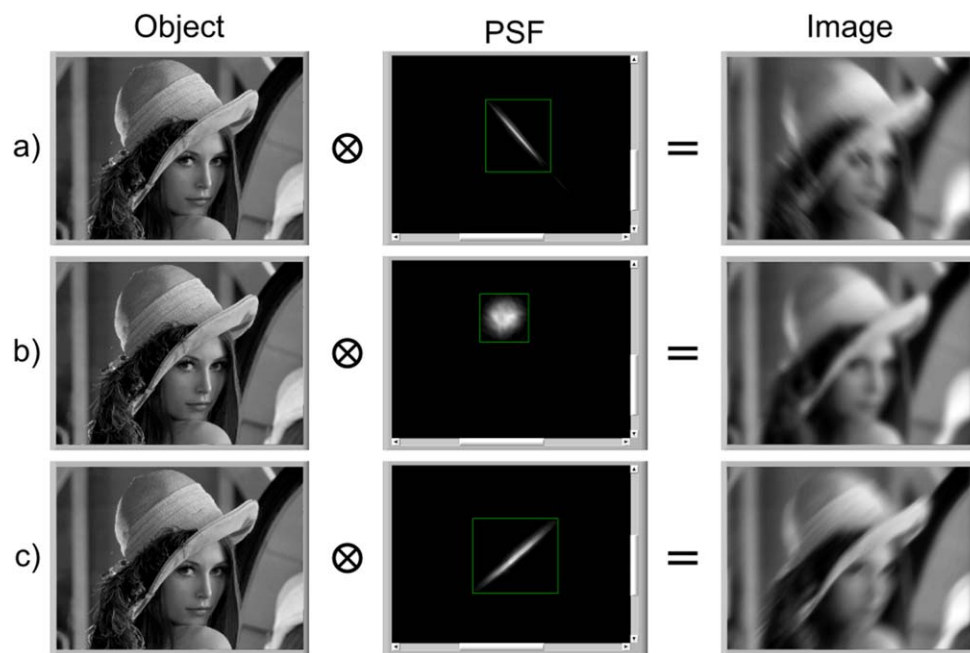


Figure 5. Experimental PSF and the simulated image for an astigmatic wavefront at three different planes along the optical axis: (a) first focal plane, (b) circle of least confusion and (c) second focal line. (c) Playboy Enterprises, Inc.

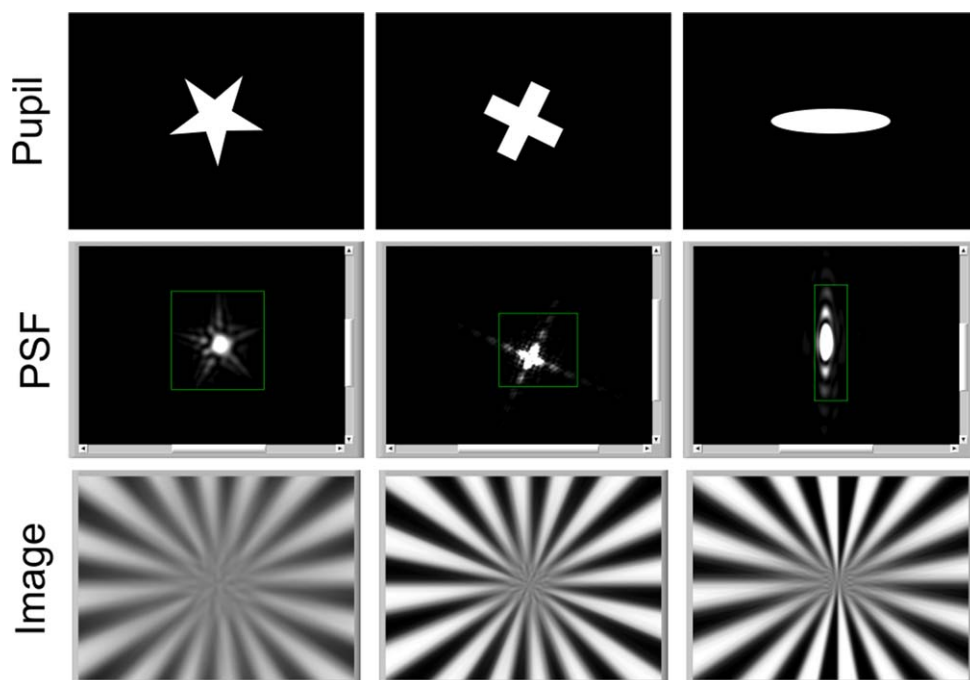


Figure 6. Effect of different pupils on the experimental PSF and on the simulated image of a Siemens Star object.

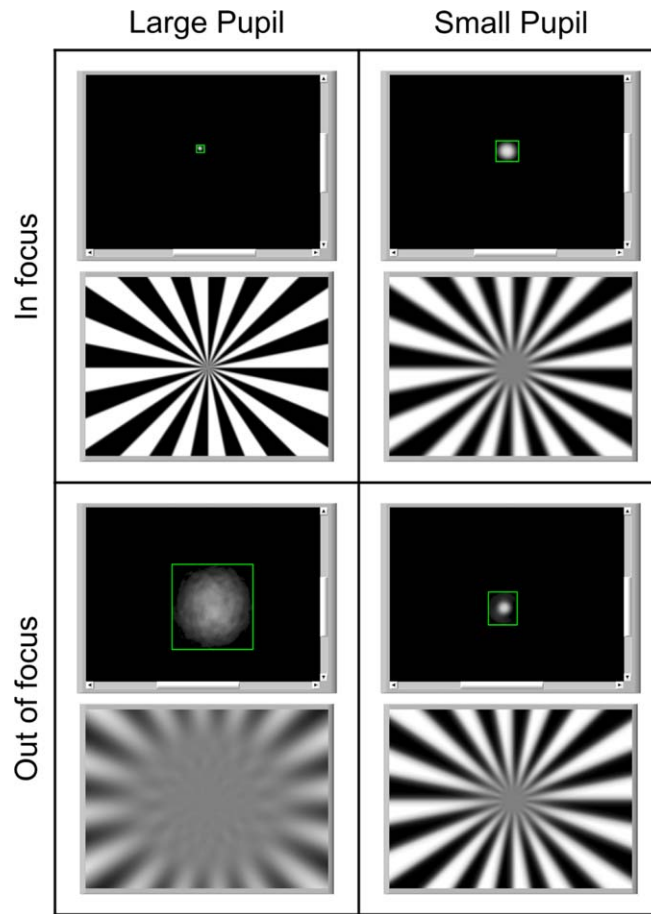


Figure 7. Study of the different DOF obtained with different pupil sizes. The green squares limits the crop area of the experimental PSFs.

the large pupil is better and the image of the Siemens star is sharper than the image provided at the same plane by the small pupil. In this case the PSF is wider due to diffraction effects (Airy pattern). However, at the defocused plane the small pupil provides a better optical quality of the image because of the extended DOF.

5. Conclusions

The PSF is an essential concept to understand the image formation properties of optical systems that are introduced theoretically in different physics courses. In this paper, an open experimental setup to measure the PSF of different elements is presented to illustrate its effect under different conditions. To avoid a tedious computational work and to show the results in real time, we have developed a LabView-based GUI. We have proposed different experiments to show the influence of the phase and the amplitude of the wavefront at the exit pupil of different OS. The proposed GUI allows one to know how a real image could be seen through the OS under study. Additionally, the proposed open experimental setup allows

students to investigate the DOF of each element. The feedback we received from the students was very positive. They found the experiment very interesting and motivating. Further, the experiment helped students to understand the basic principles of Fourier optics and digital image processing, as well as their applications in some scientific and technological areas. For example, the proposed setup can be used also to study the optical quality of multifocal lenses and the effect on the PSF of the lens tilt and decentration.

Acknowledgments

This study was supported by the Ministerio de Economía y Competitividad and FEDER (Grant DPI 2015-71256-R) and by Generalitat Valenciana (Grant PROMETEOII/2014/072), Spain.

ORCID iDs

Juan A Monsoriu  <https://orcid.org/0000-0003-3350-7951>

References

- [1] Hopkins H H 1985 Image formation by a general optical system 1: general theory *Appl. Opt.* **24** 2491–505
- [2] Marsack J D, Thibos L N and Applegate R A 2004 Metrics of optical quality derived from wave aberrations predict visual performance *J. Vis.* **23** 322–8
- [3] Born M and Wolf M 1998 *Principles of Optics* (Oxford: Pergamon)
- [4] Charrière F, Marian A, Colomb T, Marquet P and Depeursinge C 2007 Amplitude point-spread function measurement of high-NA microscope objectives by digital holographic microscopy *Opt. Lett.* **32** 2456–8
- [5] Remón L, Arias A, Calatayud A, Furlan W D and Monsoriu J A 2012 Through-focus response of multifocal intraocular lenses evaluated with a spatial light modulator *Appl. Opt.* **51** 8594–8
- [6] Goodman J W 1968 *Introduction to Fourier Optics* (San Francisco, CA: McGraw Hill)
- [7] Gaskill J D 1978 *Linear Systems, Fourier Transforms, and Optics* (New York: Wiley)
- [8] Ferran C, Bosch S and Carnicer A 2012 Design of optical systems with extended depth of field: an educational approach to wavefront coding techniques *IEEE Trans. Educ.* **55** 271–8
- [9] Ferrando V, Remón L, Pons A, Furlan W D and Monsoriu J A 2015 Wavefront sensing using a graphical user interface *Comput. Appl. Eng. Educ.* **24** 255–62
- [10] Rivera-Ortega U 2016 A simple LabVIEW-MATLAB implementation to observe the wavelength tunability of a laser diode with a diffraction grating *Comput. Appl. Eng. Educ.* **24** 365–70
- [11] Schlattauer L, Parali L, Pechousek J, Sabikoglu I, Celiktaş C, Tektas G, Novak P, Jancar A and Prochazka V 2017 Calibration of gamma-ray detectors using Gaussian photopeak fitting in the multichannel spectra with a LabVIEW-based digital system *Eur. J. Phys.* **38** 055806